© 2018 IEEE. Personal use of this material is permitted. Permission from IEEE must be obtained for all other uses, in any current or future media, including reprinting/republishing this material for advertising or promotional purposes, creating new collective works, for resale or redistribution to servers or lists, or reuse of any copyrighted component of this work in other works.

Please cite at this link: https://ieeexplore.ieee.org/abstract/document/7505299

Modeling and Identification of an Electro-Hydraulic Actuator

A. L. Cologni, M. Mazzoleni and F. Previdi[1]

***Abstract*— In this work, a physical non-linear model of an Electro-Hydraulic Actuator has been developed. Each system component (valves, pipes, cylinders) and their interactions have been modeled by means of conservation and constitutive laws. The actuator dynamics, with lumped-parameter element models, have been treated accurately, with special attention given to modeling friction. Finally, a global parametric-identification procedure has been performed for all unknown parameters. Throughout this paper all the modeling assumptions and results from system identification are verified with experimental data.**

I. INTRODUCTION

The employment of Electro-Hydraulic Actuators (EHAs) covers an important part of the actual industrial processes, such as materials presses in manufacturing machines [1]. In particular, where it is necessary to generate high forces with reduced dynamics, this solution is the most cost-effective, compared to Electro-Mechanical Actuators (EMAs), which are rather selected when precision in positioning and speed control is a tight requirement, as in [2]. Nevertheless, the use of the EMA is restricted to reduced force range with reduced lifetime mainly due to the reliability of the mechanical components that could be crucial in safety-critical applications, see for example [3]. Despite their higher reliability, the hydraulic systems present a low energy efficiency, due to the continuous running of the pump in order to keep a constant supply pressure. In order to use these equipment, a proper control law have to be defined (usually concerning speed, position or force). However, the control of such actuators is generally difficult, due to the system intrinsic non-linearities, as in [4], [5].

The strive for a continuous improvement has led to a new hydraulic actuation concept: the Electro-HydroStatic Actuators (EHSAs), reported in [6]. Recently conceived and developed, it has taken advantage from the peculiarities of both aforementioned technologies. An EHSA is a closed-circuit hydraulic transmission based on a bidirectional pump and driven by a DC brushless electrical motor, that regulates the oil flow and the pressure difference in the chambers of an hydraulic cylinder. Details about the modeling and identification of such systems can be found in [7]. Similarly to an EMA, this type of actuators can be controlled via a cascade scheme, at the cost of a bigger effort in the control design. In this view, it could be useful to resort to direct control design methods, as tested in [8].

[1]A. L. Cologni, M. Mazzoleni and F. Previdi are with Department of Management, Information and Production Engineering, Universitá degli Studi di Bergamo, 24044 Dalmine (BG), Italy alberto.cologni@unibg.it

The considered system, depicted in Fig. 1, is part of an aeronautic test bench, devoted to the analysis of EMAs which realize the imposed kinematic profile of aerodynamic surface, e.g. airplanes flaps. The component has the duty to generate a load force, simulating the resistance that the surfaces might encounter during flight.

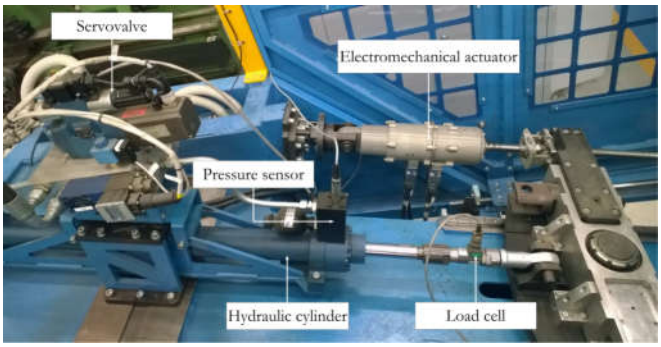

Fig. 1. The test bench with the EHA

As a principal contribution of this paper, an effective modelization of the EHA and its most common problems, due to components non-idealities, have been proposed. Once that the model has been implemented, a system identification procedure has been employed to match the simulated data with the acquired ones.

The remainder of the paper is as follows. In Section II, the hydraulic actuator features and the experimental equipment are described. Section III highlights the mathematical relations that describe the physical phenomena occurring between the system components, and the logical reasoning adopted to handle them. In section IV the identification process is outlined. Section V is devoted to the main identification results and validation performances. Finally, section VI includes conclusive remarks and possible future developments.

II. EXPERIMENTAL SETUP

The layout of the EHA considered in this work is based on a closed-circuit hydraulic transmission. The components are the traditional ones of such systems:

- a pump, actuated by an electric motor, needed to transfer mechanical energy to the oil;
- a reservoir, to hold the hydraulic fluid;
- two filters, to remove unwanted solid metal particles;
- two accumulators, preloaded with gas, in order to compensate extreme pressure demands;

- two pressure relief valves, to cope with cases in which the circuit pressure could excessively increase or decrease;
- a pilot-operated directional control valve, to route the fluid in the desired direction.

The system is activated by selecting the position, or velocity, set-point for the EMA and the desired load force for the EHA via a PC. The computer is connected to the electric drive via a SPI connection in the former case, and through a NI CompactRIO hardware in the latter. The drive deals with the control of the electric motor, while the CompactRIO compute the control law of the hydraulic one. A load cell, with $4536Kg$ of maximum force and $2\frac{mV}{V}$ of sensitivity, is mounted on the cylinder piston to close the control loop, which runs at $1kHz$.

The hydraulic actuator has a stroke of $0.860m$, with a cylinder diameter of $0.063m$ and a stem diameter of $0.036m$. A schematic system representation, along with the main considered variables and acting forces, is given in Fig. 2:

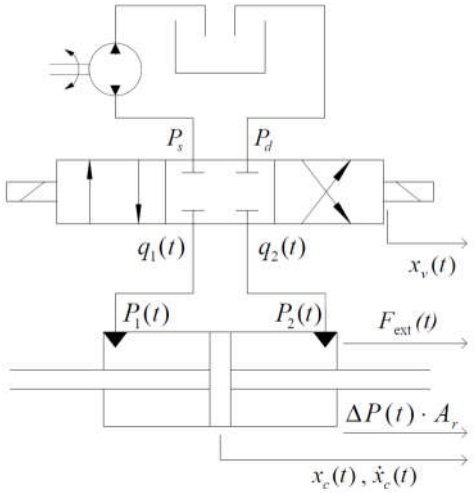

Fig. 2. Schematic of the system under study

where:

- P_s is the supply-side pressure $[Pa]$;
- P_d is the discharge-side pressure $[Pa]$;
- $q_1(t)$ and $q_2(t)$ are the outgoing flows from the valve to the cylinder $[m^3/s]$;
- $P_1(t)$ and $P_2(t)$ are the outgoing pipes pressures $[Pa]$.
- $x_c(t)$ is the cylinder position $[m]$;
- $\dot{x}_c(t)$ is the cylinder speed $[m/s]$;
- $x_v(t)$ is the valve position $[\%]$;
- A_r is the ring plate area, left free by cylinder and stem, to generate a force given a delta of pressures $[m^2]$;
- $F_{ext}(t)$ is the external force, due to the motion of the EMA connected to the EHA $[N]$.

The acquired variables, used to tune and validate the model, consist of the position and velocity of the cylinder, already acquired by the pre-existent electronic on the test bench with a $5kHz$ frequency, the valve command generated by the force regulator, and the pressures in the cylinder chambers. These last measurements have been added subsequently in order to develop the EHA model. Every measurements have been acquired at the frequency of $1kHz$ and with two I/O modules, to read both voltages and currents, each with a $16bit$ resolution. The position and the speed of the cylinder stem have been measured via a magnetostrictive linear position transducer, with $1m$ of stroke and a $0 \div 10\,V$ analog output range. The command to the valve has been acquired directly from the I/O modules mounted on the CompactRIO, while the pressures have been acquired with two analog pressure sensors, with $4 \div 20\,mA$ analog output.

After the data acquisition stage, a subsequent pre-processing stage is mandatory in order to synchronize signals measured with different sampling times, and to remove artifacts or noise components due to electro-magnetic interferences through the wired connections, via a zero-phase low-pass Butterworth filter.

III. Modeling

In this section, the model of the Electro-Hydraulic actuator is presented. The main features and the behavior of each component have been described in terms of balance equations, and the complete model is deduced.

A. Valve

The proportional valve is the component that allows to regulate the oil flows from the supply circuit to the hydraulic cylinder. Its behavior is largely described in literature, see [9]. In this document a four way (known also as $4/3$) proportional valve has been considered.

The interfaces between the valve and the external components are basically hydraulics (see Fig. 3). The component is connected, on the supply side, to a high pressure section and a reservoir via two lines both regulated in pressure. On the output side, the remaining two valve channels convey to the hydraulic cylinder chambers.

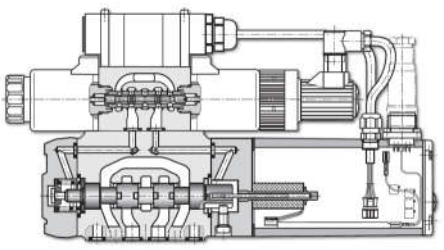

Fig. 3. Valve layout

The valve input signal (in this case $-10 \div 10\,V$) represents the stem reference position: its real position is reached through a defined dynamic. The first valve dynamic depends on its electronic: it redefines the reference, by limiting the stem speed. This behavior can be defined as follows:

$$\dot{x}_{v,r,l}(t) = \begin{cases} s_{v,max}, & \text{if } \dot{x}_{v,r}(t) > s_{v,max} \\ s_{v,min}, & \text{if } \dot{x}_{v,r}(t) < s_{v,min} \\ \dot{x}_v(t), & \text{otherwise} \end{cases} \quad (1)$$

where:

- $x_{v,r}(t)$ is the valve position reference $[\%]$;
- $s_{v,max}$ is the maximum valve speed $[\%/s]$;
- $s_{v,min}$ is the minimum valve speed $[\%/s]$;
- $x_{v,r,l}(t)$ is the limited valve position reference $[\%]$.

The limited reference $x_{v,r,l}(t)$ is used as input of the position control. The dynamic of this subsystem can be approximated as a second order low pass filter, with the following transfer function:

$$\frac{X_v(s)}{X_{v,r,l}(s)} = \frac{1}{(1+\tau_v s)^2} \tag{2}$$

where τ_v represents the time constant of the closed-loop system (usually in the order of the ms). The approximation can be conceived as pre-filtering the reference signal, by limiting its frequency content, that is, by limit the maximum signal variation.

In order to describe the relation between the stem position and the flow rates in the two outgoing pipes, it is necessary to base the equations on the analysis of the flow rate through an orifice, as written in [10]. Considering the relation between the valve position and the size of the orifice such as linear, it is possible to calculate an hypothetical flow rate through the orifice as:

$$q(t) = \frac{x_v(t)}{100} q_n \sqrt{\frac{|P_{ss} - P_{os}(t)|}{\Delta P_n}} sign(P_{ss} - P_{os}(t)) \tag{3}$$

where:

- $q(t)$ is the flow rate through the orifice $[m^3/s]$;
- q_n is the nominal flow rate of the valve $[m^3/s]$;
- P_{ss} is the pressure on the supply side that, with the considered $x_v(t)$, is connected to the output one $[Pa]$ (considered constant because, as aforementioned, regulated in pressure);
- $P_{os}(t)$ is the current pressure on the output side that, with the considered $x_v(t)$, is connected to the supply one $[Pa]$;
- ΔP_n is the nominal pressure drop of the valve $[Pa]$.

As it is possible to observe, the flow rate sign is directly related to the pressure drop of the two connected pipes.

Starting from Eq. 3, it is possible to describe the complete behavior of the valve in each configuration. The flow rates equations are grouped in Table I: in the two output lines the flows are considered positive if outgoing from the component.

TABLE Ia
FLOW RATE EQUATIONS IF $x_v(t) < 0$

Line 1	$q_1(t) = \frac{x_v(t)}{100} q_n \sqrt{\frac{\lvert P_s(t) - P_1(t)\rvert}{\Delta P_n}} sign(P_s(t) - P_1(t))$
Line 2	$q_2(t) = \frac{x_v(t)}{100} q_n \sqrt{\frac{\lvert P_d - P_2(t)\rvert}{\Delta P_n}} sign(P_d - P_2(t))$

TABLE Ib
FLOW RATE EQUATIONS IF $x_v(t) >= 0$

Line 1	$q_1(t) = \frac{x_v(t)}{100} q_n \sqrt{\frac{\lvert P_1(t) - P_d\rvert}{\Delta P_n}} sign(P_1(t) - P_d)$
Line 2	$q_2(t) = \frac{x_v(t)}{100} q_n \sqrt{\frac{\lvert P_2(t) - P_s(t)\rvert}{\Delta P_n}} sign(P_2(t) - P_s(t))$

B. Cylinder

The oil, moved from the valve, enters in the cylinder, in order to convert the hydraulic power in mechanical. The behavior of the cylinder depends basically from two phenomena:

- Pressure dynamic, derived from the compressibility of the fluid;
- Piston dynamic, related to the load, the inertia and the friction forces.

In order to determine the relation between the outgoing flow rates of the valve and the pressure in each chamber of the cylinder, it is necessary to define the flow balance equations. Considering the oil as a fluid with a constant resistance to the uniform compression, it is possible to define its bulk modulus (henceforth defined β expressed in $[Pa]$). Under this assumption, the flow rate balances are:

$$\begin{aligned} q_1(t) &= A_r \dot{x_c}(t) + c_{il}(P_1(t) - P_2(t)) + c_{el} P_1(t) + \\ &\quad + \dot{P_1}(t) \frac{V_{10} + A_r x_c(t)}{\beta} \end{aligned} \tag{4}$$

$$\begin{aligned} q_2(t) &= -A_r \dot{x_c}(t) - c_{il}(P_1(t) - P_2(t)) + c_{el} P_2(t) + \\ &\quad + \dot{P_2}(t) \frac{V_{20} - A_r x_c(t)}{\beta} \end{aligned} \tag{5}$$

where:

- c_{il} is the internal leakage coefficient $[m^3/(sPa)]$;
- c_{el} is the external leakage coefficient $[m^3/(sPa)]$;
- V_{10} and V_{20} are the oil volumes in case of $x_c(t) = 0$ $[m^3]$;
- β is the oil bulk modulus $[Pa]$.

Starting from these equation it is easy to obtain the pressure dynamic equations:

$$\dot{P_1}(t) = \frac{\beta(q_1(t) - A_r \dot{x_c}(t) - c_{il}(P_1(t) - P_2(t)) - c_{el} P_1(t))}{V_{10} + A_r x_c(t)} \tag{6}$$

$$\dot{P_2}(t) = \frac{\beta(q_2(t) + A_r \dot{x_c}(t) + c_{il}(P_1(t) - P_2(t)) - c_{el} P_2(t))}{V_{20} - A_r x_c(t)} \tag{7}$$

The last part of the cylinder description concerns the kinematic: the difference of pressure in the two chambers generates a force that, balanced with the external one, the inertia and the friction, moves the piston. Considering the

connection between the cylinder and the load as rigid, the forces law is:

$$A_r(P_1(t) - P_2(t)) = F_{frict}(\dot{x_c}(t)) + m\ddot{x_c}(t) - F_{ext}(t) \quad (8)$$

where:

- $F_{frict}(\dot{x_c}(t))$ is the friction function (depending from the piston speed) $[N]$;
- m is the moved mass $[kg]$;
- $F_{ext}(t)$ is the external force (considered in the same direction of the movement) $[N]$.

The tribology of the hydraulic cylinders is widely studied, as in [11], [12]. The most general approach considers three friction phenomena (see Fig. 4):

- Viscous friction

$$F_{frict,v}(\dot{x_c}(t)) = k_v\dot{x_c}(t) \quad (9)$$

- Coulomb friction

$$F_{frict,c}(\dot{x_c}(t)) = k_c sign(\dot{x_c}(t)) \quad (10)$$

- Stribeck friction

$$F_{frict,s}(\dot{x_c}(t)) = k_s sign(\dot{x_c}(t)) e^{-\frac{|\dot{x_c}(t)|}{\tau_s}} \quad (11)$$

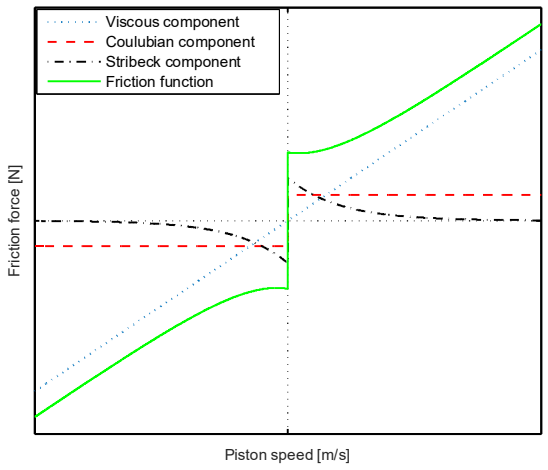

Fig. 4. Friction model

The global overall function (obtained as sum of the three components) has a discontinuity in $\dot{x_c}(t) = 0$; for this reason the real implementation of the friction model can be made:

- removing the discontinuity, using a continuous function (usually $tanh(\dot{x_c}(t))$) instead of $sign(\dot{x_c}(t))$;
- implementing a FSM (Finite-State Machine) that manages the zero passage.

In the presented work, the $tanh(\dot{x_c}(t))$ solution has been considered.

As a last consideration, it must be noted the fact that the friction coefficients could differ from a motion direction to another, that is, with the sign of the velocity. For this reason, the tribological model has been further decomposed into these two cases, leading to a new set of parameter. While the friction components functions still remain the same, the coefficients will be denoted as k_v^+, k_c^+, k_s^+, τ_s^+ when the speed is positive, and with k_v^-, k_c^-, k_s^-, τ_s^- in the opposite case. The friction forces are then computed taking into account this phenomenon.

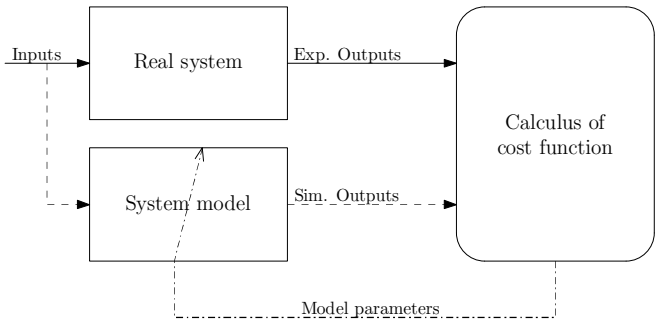

Fig. 5. Recursive identification process

C. Overall model

Considering the pipes flow rates $q_1(t)$ and $q_2(t)$ as functions of $x_v(t)$, $P_s(t)$, P_d and, respectively, $P_1(t)$ and $P_2(t)$, it is possible to describe the system in the state-space form:

$$\begin{cases} \dot{P_1}(t) = \frac{\beta(q_1(x_v(t), P_s(t), P_d, P_1(t)) - A_r s_c(t) - c_{il}(P_1(t) - P_2(t)) - c_{el} P_1(t))}{V_{10} + A_r x_c(t)} \\ \dot{P_2}(t) = \frac{\beta(q_2(x_v(t), P_s(t), P_d, P_2(t)) + A_r s_c(t) + c_{il}(P_1(t) - P_2(t)) - c_{el} P_2(t))}{V_{20} - A_r x_c(t)} \\ \dot{s_c}(t) = \frac{A_r(P_1(t) - P_2(t)) + F_{ext}(t) - F_{frict}(s_c(t))}{m} \\ \dot{x_c}(t) = s_c(t) \end{cases} \quad (12)$$

As it is described in Sections IV and V, most of the model parameters have been identified in order to simulate the system.

IV. Identification

Once a good model is obtained, it is necessary to estimate its parameters, in order to bring the simulation results as similar as possible to the experimental results. Some of the parameters can be obtained from the components features or data-sheets, while most of them have to be experimentally identified.

The identification process is usually based on the minimization of a cost function, that represents the distance between the simulated output signals and the experimental ones. In the presented case, due to the characteristics of the model (non-linear, switching), the considered algorithm is part of the iterative family methods; it means that, in order to obtain the model parameters that minimize the cost function, the algorithm must execute more than one step. The procedure, used for each step, is depicted in Fig. 5: the algorithm executes the model with the same inputs as the real system; once the simulated outputs are obtained, it is possible to calculate the cost function with the used parameters set; the algorithm, starting from the information extracted from the cost function, calculates the new parameters set and executes the next step. The used minimization algorithm is "Nelder-Mead Simplex Method", and its convergence properties are

demonstrated in [13]. The Nelder-Mead method attempts to minimize a scalar-valued nonlinear function of n real variables using only function values, without any derivative information, being thus a direct optimization method. The algorithm maintains at each step a nondegenerate simplex, a geometric figure in n dimensions of nonzero volume that is the convex hull of $n+1$ vertices. Each iteration of a simplex-based direct search method begins with a simplex, specified by its $n+1$ vertices and the associated function values. One or more test points are computed, along with their function values, and the iteration terminates with a new (different) simplex such that the function values at its vertices satisfy some form of descent condition compared to the previous simplex.

One of the key-points of the identification process is the definition of the cost function. In the presented work, the acquired signals are: $P_1(t)$, $P_2(t)$ and $\dot{x}_c(t)$ (the rod position hasn't been used in the cost function because directly related to the speed). The considered variables are, obviously, defined as discrete time signals: for this reason the time index (defined above as t) has been replaced by k. The complete cost function is:

$$J = \sum_{k=1}^{N} \frac{1}{N} \left(\left(\frac{P_1(k) - P_{1,s}(k)}{max(P_1(k))} \right)^2 + \left(\frac{P_2(k) - P_{2,s}(k)}{max(P_2(k))} \right)^2 + \left(\frac{\dot{x}_c(k) - \dot{x}_{c,s}(k)}{max(\dot{x}_c(k))} \right)^2 \right) \quad (13)$$

The training procedure used 91300 points, while 135722 points were used for the validation phase.

The identified parameters are: $\frac{q_n}{\sqrt{\Delta P_n}}$, β, V_{10}, V_{20}, c_{il}, c_{el}, m, k_v^+, k_v^-, k_c^+, k_c^-, k_s^+, k_s^-, τ_s^+ and τ_s^-.

V. Results

In order to verify the developed model, a set of experiments has been done on the real system. A part of the acquired data have been used in order to identify the model parameters, while the other acquisition are used for the validation of the model.

In order to quantify the quality of the tracking, the ESR (Error to Signal Rate) is computed using the following equation:

$$ESR = 100 \cdot \sum_{t=1}^{N} \frac{\text{Var}[y(t) - y_s(t)]}{\text{Var}[y(t)]} \quad (14)$$

where:

- N is the number of measured samples;
- t is the time index;
- Var$[x]$ of the variance operator for a signal x.

The considered input signals are $x_v(t)$, $F_{ext}(t)$ and $P_s(t)$ (see Figure 6). The outputs are $\Delta P(t) = P_1(t) - P_2(t)$ and $\dot{x}_c(t)$.

The identified parameters values are:

- $\frac{q_n}{\sqrt{\Delta P_n}} = 4.68 \cdot 10^{-7}\, m^4/\sqrt{kg \cdot m}$;
- $\beta = 1.73 \cdot 10^9\, Pa$;
- $V_{10} = 2.11 \cdot 10^{-4}\, m^3$;
- $V_{20} = 6.75 \cdot 10^{-4}\, m^3$;
- $c_{il} = 2.18 \cdot 10^{-11}\, m^3/s \cdot Pa$;
- $c_{el} = 0\, m^3/s \cdot Pa$;
- $m = 74.11\, kg$;
- $k_v^+ = 1.21 \cdot 10^4\, kg/s$;
- $k_v^- = 1.37 \cdot 10^4\, kg/s$;
- $k_c^+ = 1.14 \cdot 10^3\, N$;
- $k_c^- = 1.18 \cdot 10^3\, N$;
- $k_s^+ = 244.37\, N$;
- $k_s^- = 39.36\, N$;
- $\tau_s^+ = 3.41 \cdot 10^{-3}\, m/s$;
- $\tau_s^- = 1.96 \cdot 10^{-3}\, m/s$.

The identification results are depicted in Figure 7, while their ESR quantifications are summarized in Table II.

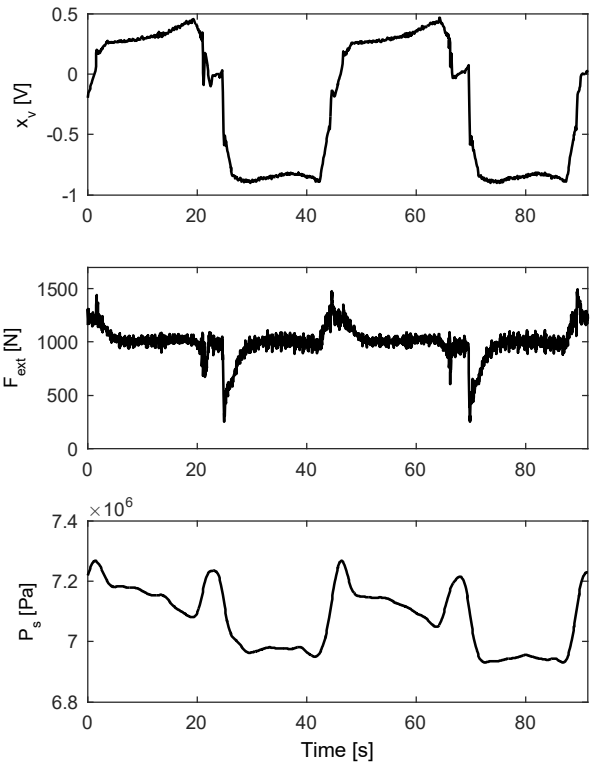

Fig. 6. Identification inputs

In order to validate the model, another experiment has been carried out with the identified parameters and a different load profile. As it is possible to observe (see Figure 8) the model is valid also in these conditions: the ESRs for this trial are reported in Table III.

VI. Conclusions and Future Devleopment

In this paper a non-linear model of an Electro-Hydraulic actuator, installed on a aeronautic test bench, has been presented. The proposed model is developed merging the dynamic equations of each component of the system. In

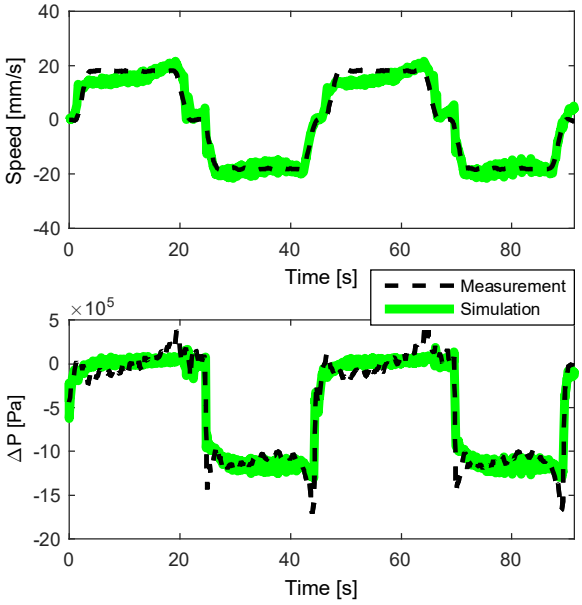

Fig. 7. Identification results

TABLE II
IDENTIFICATION RESULTS

	$\Delta P(t)$	$\dot{x}_c(t)$
ESR %	4.98	3.39

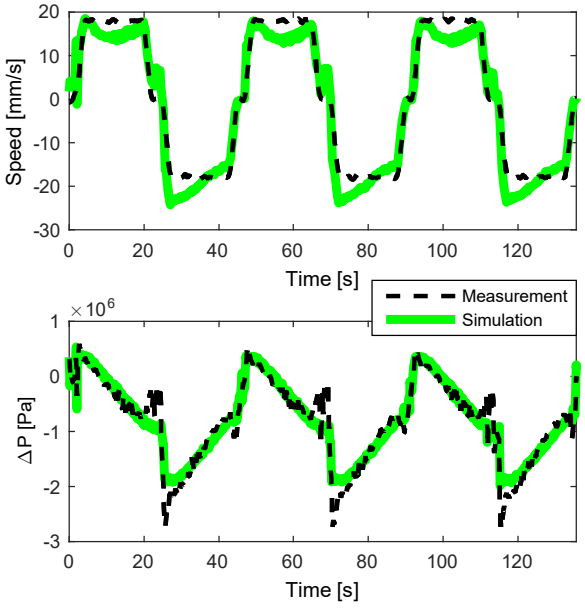

Fig. 8. Validation results

TABLE III
VALIDATION RESULTS

	$\Delta P(t)$	$\dot{x}_c(t)$
ESR %	9.21	4.37

order to test the goodness of the proposed solution, the model has been implemented in a simulation software and an identification of its parameters has been carried out using experimental acquisitions. The efficacy of the model and of the identification is proved by the comparison between simulation results and experimental data.

ACKNOWLEDGMENT

This research activity has been carried out in the context of the research project *HOLMES* funded by CleanSky Joint Technology Initiative.

REFERENCES

[1] S. Engleder, "Time-optimal motion planning and control of an electrohydraulically actuated toggle mechanism," *Mechatronics*, vol. 17, no. 8, pp. 448–456, 2007.
[2] R. Isermann and U. Raab, "Intelligent actuators ways to autonomous actuating systems," *Automatica*, vol. 29, no. 5, pp. 1315–1331, 1993.
[3] E. Balaban, P. Bansal, P. Stoelting, A. Saxena, K. F. Goebel, and S. Curran, "A diagnostic approach for electro-mechanical actuators in aerospace systems," in *Aerospace conference, 2009 IEEE*. IEEE, 2009, pp. 1–13.
[4] C. Guan and S. Pan, "Nonlinear adaptive robust control of single rod electro hydraulic actuator with unknown nonlinear parameters," *Control Systems Technology, IEEE Transactions on*, vol. 16, no. 3, pp. 434–445, 2008.
[5] G. A. Sohl and J. E. Bobrow, "Experiments and simulations on the nonlinear control of a hydraulic servosystem," *Control Systems Technology, IEEE Transactions on*, vol. 7, no. 2, pp. 238–247, 1999.
[6] S. Habibi and A. Goldenberg, "Design of a new high performance electrohydraulic actuator," in *Advanced Intelligent Mechatronics, 1999. Proceedings. 1999 IEEE/ASME International Conference on*. IEEE, 1999, pp. 227–232.
[7] D. Belloli, F. Previdi, S. Savaresi, A. Cologni, and M. Zappella, "Modeling and identification of an electro-hydrostatic actuator," in *Mechatronic Systems*, 2010, pp. 620–625.
[8] S. Formentin, A. Cologni, D. Belloli, F. Previdi, and S. M. Savaresi, "Fast tuning of cascade control systems," in *IFAC World Congress*, vol. 18, 2011, pp. 10 243–10 248.
[9] H. E. Merritt, *Hydraulic control systems*. John Wiley & Sons, 1967.
[10] G. Diana and F. Resta, *Controllo di sistemi meccanici*. Polipress, 2007.
[11] P. Drumea, C. Cristescu, A. Fatu, and M. Hajjam, "Experimental research for measuring friction forces from rod sealing at the hydraulic cylinders," *Annals of" Dunarea de Jos" University Galati. Fascicle VIII, Tribology*, vol. 16, no. 2, pp. 10–14, 2010.
[12] B. Bhushan, *Modern Tribology Handbook, Two Volume Set*. CRC Press, 2010.
[13] J. C. Lagarias, J. A. Reeds, M. H. Wright, and P. E. Wright, "Convergence properties of the nelder–mead simplex method in low dimensions," *SIAM Journal on optimization*, vol. 9, no. 1, pp. 112–147, 1998.